ISTITUTO NAZIONALE DI FISICA NUCLEARE

Sezione di Milano

FEATURES OF A PHASE-ONLY SHAPER RELATIVE TO A LONG RECTANGULAR ULTRAVIOLET PULSE

Simone Cialdi, Ilario Boscolo and Alessandro Flacco[1]

[1])*University and INFN, via Celoria 16, 20133 Milano, Italy*

Abstract

The generation of a very low-emittance high peak charge electron beam in a 3-GHz radiofrequency electron gun requires a rectangular shaped electron beam of 10 ps with a rise time less than 1 ps at the cathode surface. This is obtained illuminating a photocathode with a powerful ultraviolet laser pulse of that form. A programmable pulse shaper is added into the chain of the components of a femtosecond solid-state laser system for producing such a kind of pulse. The shaping system operates as a spectral phase-only filter. A genetic algorithm, in conjunction with a proper cost-function, is used to determine the phase function to be set in the shaper for generating the square pulse matching the specifications. The simulations show that the system is very sensitive to the signal parameters and alignment. The simulations show that the output signals at the fundamental and third harmonic have differences relevant for the setting of the system

Submitted to J. Opt. Soc. of Am.B

1   Introduction

The development of low-emittance (few π mm-mrad) electron sources is required for application in X-UV free electron lasers (FELs) [1–3], Compton scattering [4] and new generation of linear colliders [5]. The study of our SPARC [1] (Sorgente Pulsata e Amplificata di Radiazione Coerente) FEL experiment has shown the necessity of an electron beam of $\approx 1\,\pi\,mm - mrad$ [7]. This requirement means a radiofrequency electron gun (rf-gun) whose photocathode is driven by a UV laser rectangular pulse of 10 ps with a fraction of 1 ps rise time. In fact, it was shown also experimentally that the emittance depends on the temporal laser pulse characteristics and that its minimum value is reached with a rectangular pulse having the above written characteristics [6].
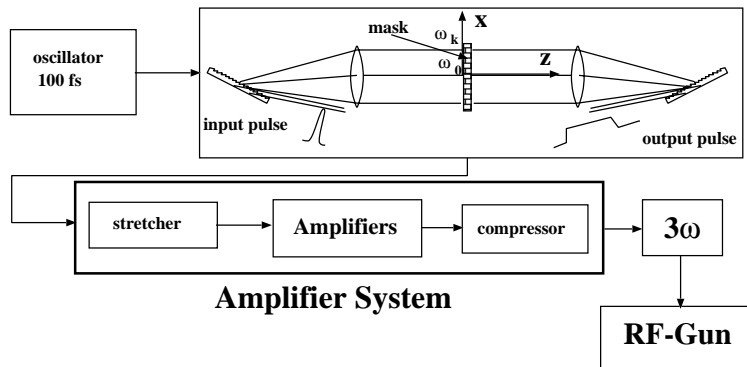

Figure 1: Sketch of the system layout with the pulse shaper insertion.

The generation of a rectangular light pulse is obtained by a laser system composed of an oscillator and a system of amplifiers with in between a temporal pulse shaper. The oscillator delivers a very short pulse, less than 1 ps, the shaping system performs the transformation of that Gaussian pulse into a rectangular one. Systems for manipulating sub-picosecond pulses with the aim of generating complicated ultrafast optical waveforms and relatively long square pulses according to user specifications are studied and tested since a decade [8–11]. In this article we consider the so-called 4-f-grating-lens shaper [9,12], see Fig. 1. In this system the spectrum components of the incident light pulse are firstly spatially dispersed by a grating, then a lens transforms the dispersed rays into spots at the transform plane, here a filter mask, see Fig. 2 makes the desired filtering action on the light beam (provides the desired shape), then a second lens transforms back the component rays into a convergent pulse and, finally, a second grating synthesizes the components into the long square pulse. The mask is called Liquid Crystal Programmable Spatial Light Modulator, called LCP-SLM [9].

In this article we present the rationale of producing a 10 ps pulse, as flat as pos-
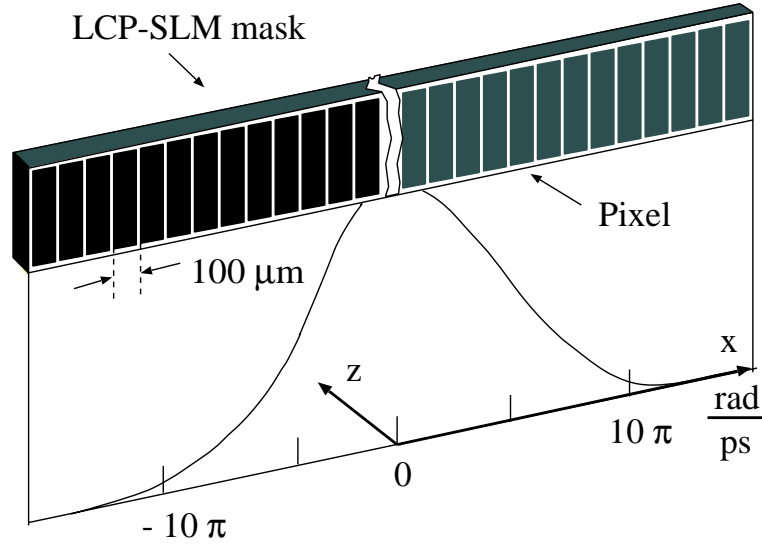
Figure 2: Sketch of the mask layout with the spectral part of the input gaussian signal crossing the mask.

sible at the third harmonic, starting from a typical 100 fs (which can be provided by a Ti:sapphire cw oscillator). The photoemission from a metallic cathode, as programmed in SPARC system (and many others), requires the photon energy of the third harmonic of a Ti:sapphire 800 nm laser [1,2].

2   A phase-only shaper for square intensity pulses

The femtosecond pulse shaping is a linear filtering process. In the time domain the filter action of the shaper is represented by the *impulse response function* $h(t)$, while in the frequency domain the filter action is represented by the Fourier transform $H(\omega)$ of $h(t)$. The output waveform $e_{out}(t)$ is the convolution of the input waveform $e_{in}(t)$ and the impulse response function h(t)

$$e_{out}(t) \;=\; h(t) * e_{in}(t) \tag{1}$$

In the frequency domain we may write

$$E_{out}(\omega) \;=\; H(\omega) \cdot E_{in}(\omega) \tag{2}$$

The mask of a LCP-SLM shaping system is patterned as an array of pixels (typically 97 μm wide) interleaved with small gaps ($\sim 3\ \mu m$ wide). Because of the mask pixellation, Eq. 1 is changed into [13]

$$e_{out}(t) \;\cong\; \left[\sum_{n} h(t - n\frac{1}{\delta\nu}) * e_{in}(t) \right] \cdot \frac{sin(\pi\delta\nu\, t)}{\pi\delta\nu\, t} \tag{3}$$

3

The spectral width $\delta\nu$ is relative to the individual pixel of width $\delta x = 2\pi\alpha\delta\nu$ where α is the spatial dispersion of the beam components. The expression (3) assumes negligibly small interpixel gaps and a focused spot size w_0 at the masking plane less than the pixel dimension. The result of the pixellation is to produce an output pulse which is the convolution of the input pulse not only with the desired impulse response function h(t), but also with a series of replica impulse response functions, $h(t - n\delta\nu^{-1})$, occurring at times $t = n\delta\nu^{-1}$. The entire result is weighted by a temporal window function, $sinc(\pi\delta\nu t)$, which has the first zeros at $t = \pm\delta\nu^{-1}$. However, in our problem of obtaining a square intensity pulse at UV, i.e. after the frequency multiplication, the lateral replica become vanishingly small, therefore negligible.

In order to define the impulse response function $h(t)$ and its Fourier transform $H(\omega)$, we observe that the dispersion law, in quite good approximation, is $x \cong \alpha\,\omega$ (is referred to the central frequency ω_0), and we may assume a beam waist w_0 of the spectral components at the mask plane such that only the lowest Hermite-Gaussian mode is filtered [14]. The response function ends up to be [9,14]

$$H(\omega) = \sqrt{\frac{2\alpha^2}{\pi\,w_0^2}}\,H_{SLM}(\omega) * e^{-2\,\frac{\alpha^2}{w_0^2}\,\omega^2} \tag{4}$$

The effect of the convolution of the pixellated response function $H_{SLM}(\omega)$ with the envelope function $e^{-2\,\alpha^2\omega^2/w_0^2}$ is a smoothing of the pixellated response. Therefore, when w_0 is minor than the pixel width the smoothing effect is negligible, when the beam waist is comparable with the pixel dimension the suppression of the lateral replica occurs. The case of w_0 larger than the pixel dimension must be avoided because the output pulse is negatively affected. However, again because of the third harmonic interest, we do not have to match the condition of beam waist about the pixel width.

A complete LCP-SLM induces both a phase and amplitude modulations. Hence, the general frequency response function $H_{SLM}(\omega)$ is characterized by its amplitude modulation $M(\omega)$ and spectral phase $\Phi(\omega)$, that is

$$H_{SLM}(\omega) = M(\omega)\,e^{i\,\Phi(\omega)} \tag{5}$$

However, since in our problem only the temporal intensity profile is requested, we have the degree of freedom of choosing phase-only filters. In fact, the time domain intensity (and amplitude) is specified but the temporal phases are free. Besides, the shaped pulse must be highly amplified (a high energy per pulse is required by a metallic photocathode in order to deliver the wanted one nano-Coulomb charge), hence it is important to have a large spectrum in order to have a pulse stretching enough long into the amplifiers so to avoid optics damage [8].

Choosing the phase-only filtering and the beam waist w_0 minor than the pixel dimension the spectral amplitudes of the input and output signals can be assumed the same. Therefore, $H_{SLM}(\omega) = exp[i\,\Phi(\omega)]$. In this case an analytical solution does not generally exist, but many numerical solutions for the phase modulation function $\Phi(\omega)$ satisfactory enough can be found. A computer assisted calculation can find a spectral phase distribution which leads to an output pulse which approximates fairly well the target pulse.

For the above purpose we have developed a computer program (in C++ language). The wanted transfer function of a programmable mask is found applying an iterative Fourier transform algorithm: the spectral pattern programmed into the pulse shaper is updated interactively according to a Genetic stochastic optimization Algorithm (GA) based on the difference between the desired and the wanted output [15,16]. The calculation procedure is illustrated in Fig. 3

The complex spectral field $E(\omega)$ of the input pulse (characterized by its spectral amplitude and phase $A(\omega)$ and $\phi(\omega)$) and the temporal amplitude z(t) of the target pulse are given as inputs.

The calculation begins by settings a zero phase delay to an initial trial phase vector Φ. In each iteration a random phase change $\delta\Phi_i$ is generated according to $\delta\Phi_i = R$ where R is a random variable uniformly distributed in the interval $-0.5 \div +0.5$ and the index i refers to the i-th pixel. At the end of each iteration a $cost - function$ provides a measure of the deviation of the output pulse from the target pulse. The new spectral phase function is accepted by the program if the $refreshed\,cost - function$ calculated with the new spectral phase function results smaller than that calculated with the last accepted spectral phase function. It is otherwise rejected. There are many kinds of $cost - functions$ and the choice of it is determined by the particular target waveform [16,17]. The stop of the iteration occurs when the value of the $cost - function$ arrives at its saturation. The final phase pattern $\Phi(\omega) - \phi(\omega)$ is transferred to the mask.

In our case of long rectangular pulse, the choice of the $cost - function$ came out to be very important. We found, see next section, a dependence of the flatness on the $cost - function$ type.

3 The choice of the cost-function, the target pulse rise time and the beam waist at the mask

We have applied our simulation program, based on the genetic algorithm, to a mask of 640 pixels of 100 μm width (Jenoptics company) illuminated by an input gaussian pulse of 100 fs. The pulse conveyed through the mask was truncated to a spectral width equal to $30\,\pi$ rad/ps. The target pulse was obviously 10 ps with a rise time less than 1 ps. As
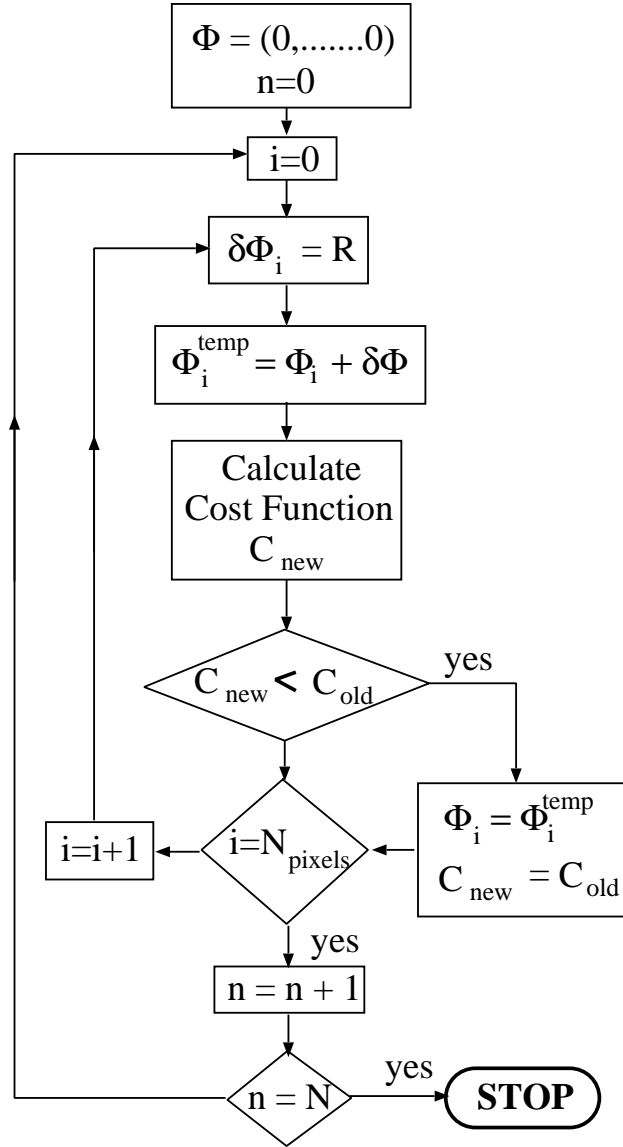
Figure 3: Scheme of the iterative Fourier transform algorithm (FT = Fourier Transform).

we see just below the rise time and the plateau flatness resulted related.

The first problem we have considered was the choice of the $cost-function$. In Fig. 4 are depicted the computed temporal intensity profiles of the output pulse after the application of the iterative algorithm with the following two $cost-functions$

$$C_1 = \sum_n |I_n - I_n^{target}| \tag{6}$$

$$C_2 = \sum_n (I_n - I_n^{target})^2. \tag{7}$$

The mask patterns found with the two different $cost-functions$ lead to quite differ-
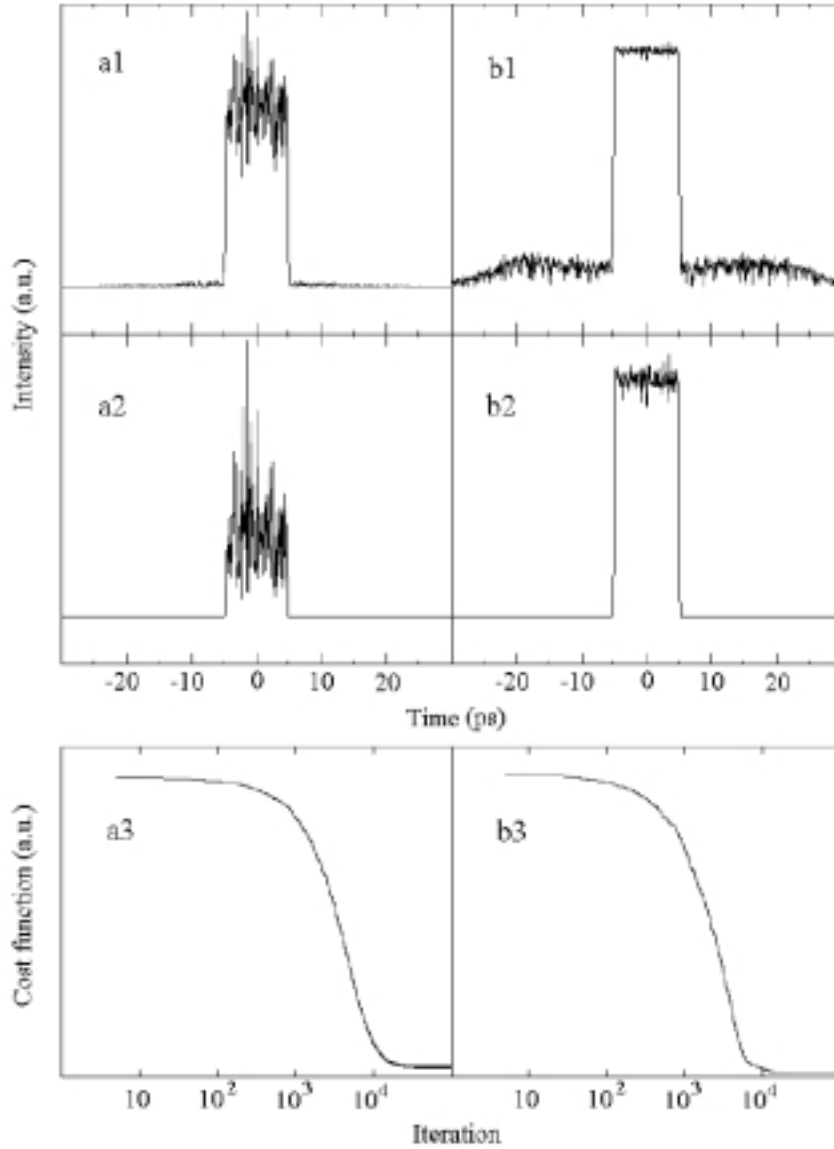
6

Figure 4: Simulated output pulses after the shaper obtained with the iterative algorithm: The signals of frames a1 and b1 refer to the fundamental harmonic and are obtained with the $cost-function\ C_1$ and C_2 respectively. The two a2 and b2 frames refer to the 3rd harmonic. The lower frames show the behavior of the two $cost-functions$ with the number of iterations.

ent output signals for both the fundamental and third harmonics: The $cost-function\ C_1$ leads to a much more spiky signals at the flat top. The spiking is amplified in the process of third harmonic up-conversion (as expected by the non-linearity of the process), but, positively, the fluctuations at the signal sides are cut off. The $cost-function$ $C_3 = \sum_n [I_n^2 - (I_n^{target})^2]$ (chosen for its strong sensitivity to the intensity oscillations at the plateau and, instead, low sensitivity to the intensity oscillations at the tails) failed as tool for the simulation. The $C_4 = \sum_n |I_n - I_n^{target}|^3$ (which has a power increment

7

of a unity with respect to C_2) showed to be a bit worse than the $cost - function\, C_2$. The $C_2\, cost - function$ of Eq. 7 has to be chosen. The simulation relative to the third harmonic intensity is calculated by the cubic power of the first harmonic intensity.
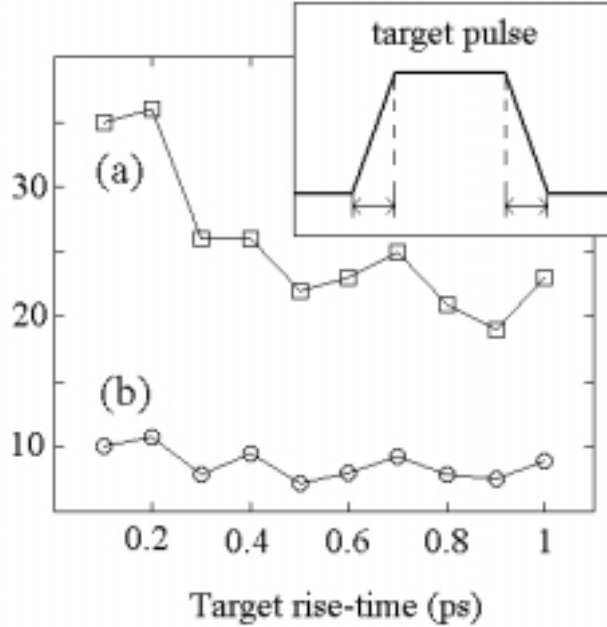

Figure 5: The upper line represents the ratio of the spiking amplitude at the flat top over the mean value, i.e. $(I_{max} - I_{min})/I_{average}$, as function of the rise time, the lower curve represents the ratio of the standard deviation over the mean, i.e. $[2\,\sigma/I_{av}]$, as function of the rise time.

The second issue to make a trade off is the signal rise time. This has to be the shortest as possible (anyway shorter than 1 ps for low emittance purpose). The simulations, see Fig. 5, show that the lower the rise time the higher the spiking in the flat-top. The spiking amplitude reaches about 30% with a rise time around 200 ps. At half a picosecond the deviation from the average value is nearby the minimum, hence we choose that rise time as reference value for the target pulse. A longer risetime would worsen the electron beam emittance.

The issue to investigate, at last, is the proper dimension of the beam waist at the mask. We did the simulations with the three following values: 100, 60 and 20 μm. In Fig. 6 the results, that is the output signals on the fundamental harmonic, are reported. We notice that the larger w_0 the lower are both the noise-like bumps at the sides, the opposite for the flatness. About this issue we observe that the swellings at the tails are cut down by the harmonic conversion. Thus, we decide to choose for now on $w_0 = 20\,\mu m$. We remark that we have done the simulations for all the beam waist dimensions assuming the fundamental mode only. This is allowed because a regenerative amplifier follows the
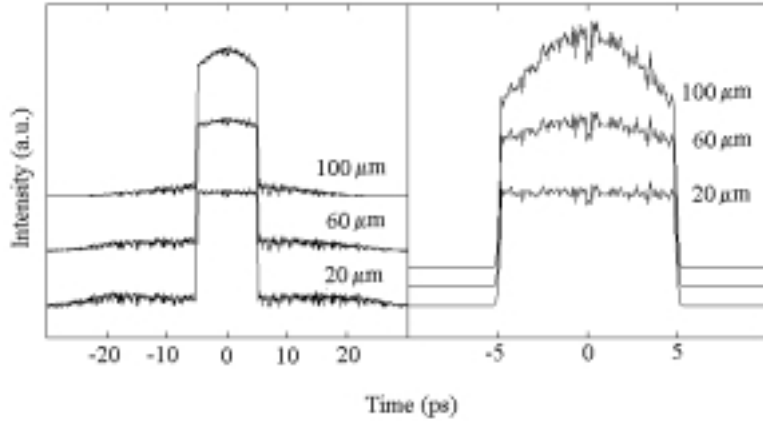
Figure 6: The left and right frames report respectively the variation of the calculated output pulse versus the variation of the beam waist at the mask for the first and third harmonics.In the calculation we have considered only the lowest Hermite-Gaussian mode for every beam waist. The replica are at 42 ps thus outside the reported time interval. They are anyway such a small to be neglectable.

shaper and it does the appropriate spatial filtering.

4   The results relevant for our system

We present now the variations on the output signals brought about by the deviations of the input signal parameters, that is pulse length, beam alignment, mask position and finally beam shape. The simulations are done applying to the different cases the spectral patterned function $\Phi(\omega)$ found for the reference input pulse (100 fs and gaussian shape) and reference shaper parameters ($w_0 = 20\,\mu m$ and centered spectral bandwidth through the mask of $30\,\pi\,rad/ps$). The shift of the central frequency (possibly due to a laser instability) should seemingly produce an effect on the output similar to the shift of the mask along the x-axis direction. In fact, a shift of the central frequency leads on one side of the mask an exit of a frequency interval and on the opposite side of the mask an entrance of an equivalent spectral interval of the other side of the spectrum. The results of the simulation are depicted in Figs. 7 and 8.

- *Pulse length deviation of 5 fs*. If the pulse length moves towards either 95 or 105 fs instead of the reference 100 fs, the spiking amplitude $(I_{max} - I_{min})/I_{average}$ on the third harmonic at the flat top increases from 20 % to ~ 80 %.

- *Shift of the mask of 0.5 mm with respect the central position*. The spiking enhancement arrives up to the ~ 70 %.

- *Shift of the incident angle θ_i*. Since a variation of θ_i induces a variation on α (because of the grating action the spatial dispersion α depends on the diffracted angle
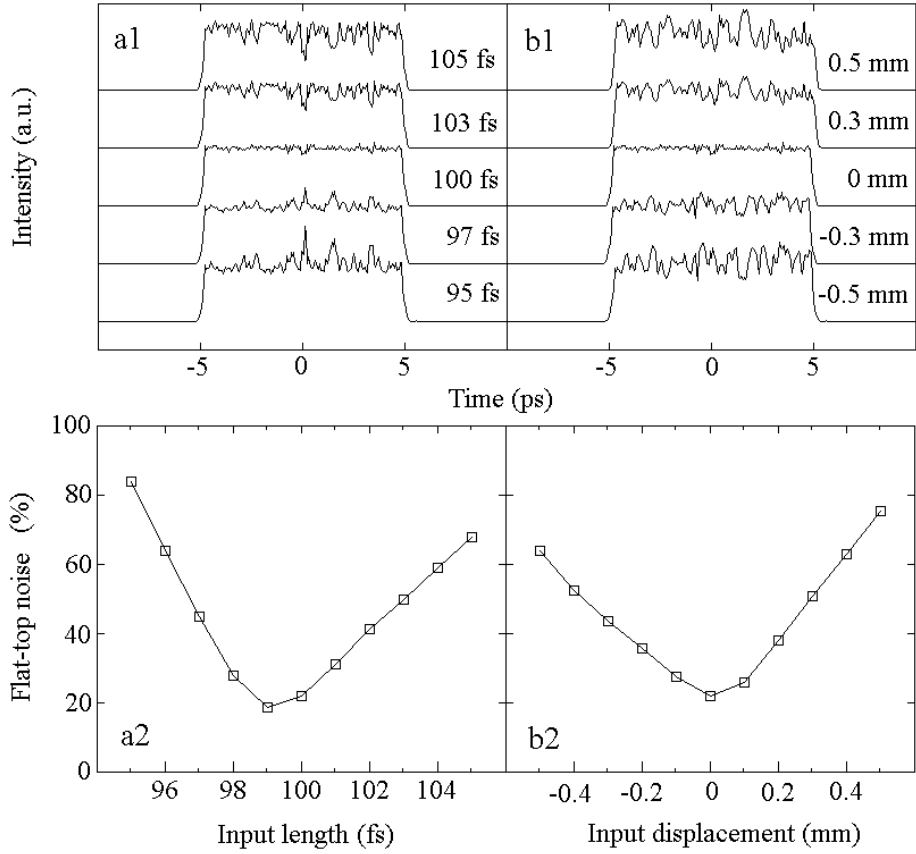
9

Figure 7: The upper frames report the variation of the calculated output pulse on the third harmonic versus the variation of the pulse length (left frame) and shift from the centered position of the mask. The lower panels show the relative behavior of the the spiking amplitude over the mean value, i.e. $(I_{max} - I_{min})/I_{average}$, as function of the length and mask position deviations.
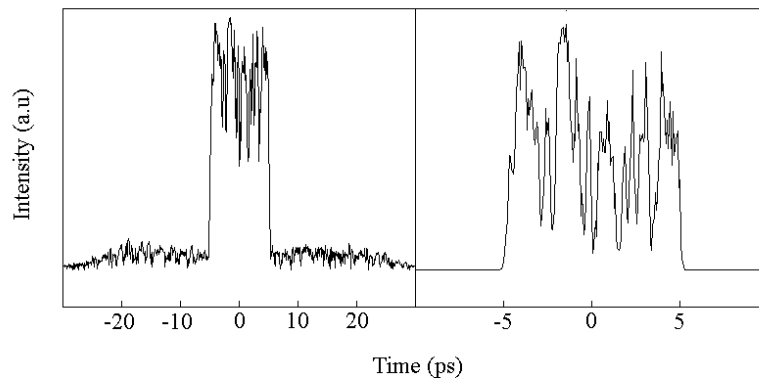

Figure 8: The left and right frames report respectively the calculated output pulses for the first and third harmonics assuming a hyperbolic secant function for the input pulse instead of the gaussian function. The flatness is practically lost.

10

θ_d, which in turn is a function of θ_i, i.e. $\alpha \propto 1/cos\,\theta_d(\theta_i)$ [9]) the spectral bandwidth hitting the mask is changed. This can easily seen looking at the expression of the spectral intensity at the mask

$$I(x) = e^{-\frac{\tau^2}{2\cdot(1.177)^2}\cdot\frac{x^2}{\alpha^2}}$$ (8)

where τ is the time pulse width. A small variation of α about the reference value induces a variation on the spectral intensity $I(x)$ analogous to that induced by the variation of the pulse length τ. Therefore, the previously seen results relative to the pulse length deviation can be extended to the case of θ_i small deviation: The 30 % spiking enhancement means a 2 % α variation.

- *The change of the pulse shape*. In passing from the Gaussian shape to the hyperbolic secant shape (as possible for a mode locked oscillator) the reduction of the flatness is dramatic, see Fig. 8.

The high sensitivity of the system to variations of the input pulse length is due to the technique of the phase-only shaping in the condition of wide spectral acceptance, see Fig. 9. In fact, we have checked that the wider is the spectral acceptance the higher both the pulse flatness and the system sensitivity to any variation. It could be advisable to choose a less portion of the spectral bandwidth, so, in turn, to accept a worse flatness, for having a less sensitivity to small deviations of the pulse length. The spectral components under the signal tails are important for smoothing down the roughness of the pulse plateau with their right phase position, but the puzzle of the phases is very tight, a small change brings about a large change. The strong enhancement of the oscillations at the flat top of the output signal when the input signal changes its shape, is seemingly due to the relatively high amplitude variation of the spectral components interested by the shape variation. To limit the high sensitivity the combination of phase and amplitude modulations, compatible with the amplifying system requirements, should be applied.

Powerful laser amplifiers introduce large group-delay dispersion [8,18]. A shaper system should recover the pulse deformations. This is a good reason for having a flexible, that is programmable, shaper system in those lasers.

5   Conclusions

We have shown with computer simulations based on a genetic algorithm that a 100 fs pulse can be transformed into a rectangular pulse of 10 ps with 0.5 ps rise time using a phase-only shaping filter. A satisfactory result about the pulse flatness requires an appropriate
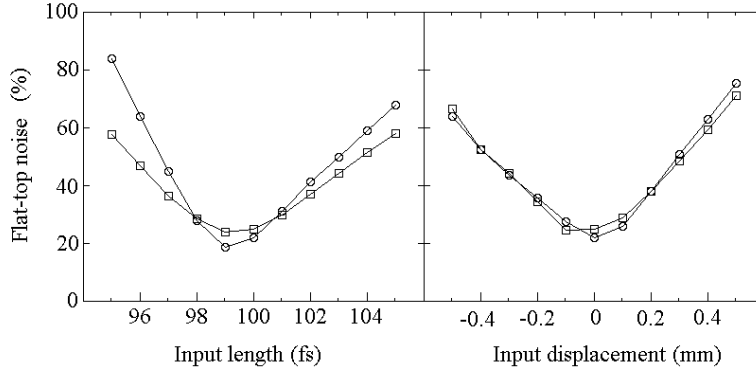
Figure 9: Left frame shows the variation of the plateau flatness with the perturbation of the pulse length for the reference $30\,\pi$ spectral bandwidth through the mask (line with circles) and for a reduced acceptance of 3/4 of that reference acceptance (line with squares). We notice that the latter is less sensitive to the lenght perturbations. The right refers to the perturbations of the mask position. The sensitivity does not change, as expected.

$cost - function$ within the computer program. Conditions for a good flatness are a rise time higher than 0.5 ps and a beam waist at the mask of the shaper about 1/5 the dimension of the mask pixel and a wide spectral acceptance of the mask. The system shows to be very sensitive to both the variations of the input pulse characteristics and to the alignment. A way to get partially round of the tight requirement on the system stability is to reduce the requirement on the flatness, so to reduce the spectral acceptance. Our SPARC project fortunately can accept oscillations at the plateau up to the notable value of 30% peak-to-peak. A less sensitive shaping system seems possible exploiting a combination of phase and amplitude modulations. The amplitude modulation must be compatible with the amplifying system requirements. The work will be published in a next papers.

The spiking on the plateau are amplified by the conversion into the third harmonic. On the other side, in this case the fluctuations on the tails of the signal in the first harmonic are suppressed. This must be taken into account when the UV radiation is requested.

References

[1] SPARC "Conceptual design of a high-brightness linac for soft X-ray SASE FEL source," EPAC 2002 (La Villette, Paris) 5 June 2002.

[2] M. Cornacchia et al., "Linac coherent light source (LCLS) design study report" (Stanford University-University of California) Report No. SLAC-R-521/UC-414, revised 1998.

[3] F. Richard et al, "TESLA, the superconducting electron-positron linear collider with an integrated X-ray laser laboratory, technical design report," Desy Report No. DESY2001-011, ISBN 3-935702-00-0, 2001

[4] P. T. Springer et al, "Ultrafast Material probing With the Falcon/Linac Thomson X-ray Source" 2002.

[5] J. Yang, M. Washio, A. Endo and T. Hori, Nuc. Inst. Methods Phys. Res. A **428** 556–569 (1999).

[6] J. Yang, F. Sakai, T. Yanagida, M. Yorozu, Y. Okada, K. Takasago, A. Endo, A. Yada, and M. Washio, J. Appl. Phys. **92,** 1608–1612 (2002).

[7] M. Ferrario, M. Boscolo, V. Fusco, C. Vaccarezza, C. Roncisvalle, J. B. Rosenzweig and L. Serafini, "Recent advances and novel ideas for high brightness electron beam production based on photo-injectors," Invited talk at the ICFA Workshop on "The physics and application of high brightness electron beams" (Chia Laguna, Sardinia, Italy) 1–6 July 2002.

[8] S. Backus, C. G. Durfee III, M. M. Murname and H. C. Kapteyn, Rev. Sci. Instrum. **69,** 1207–1223 (1998).

[9] A. M. Weiner, Rev. Sci. Instrum., **71,** 1929–1960 (2000).

[10] P. Tournois, Opt. Commun. **140,** 245–249 (1997).

[11] F. Verluise, V. Launde, J-P. Huignard, P. Tournois, and A. Migus, J. Opt. Soc. Am. B. **17,** 138–145 (2000).

[12] A. M. Weiner, D. E. Leaiard, J. S. Patel and J. R. Wullert, IEEE J. Quantum Electron, **284,** 908–920 (1992).

[13] M. M. Wefers and K. A. Nelson, J. Opt. Soc. Am. B **127,** 1343–1362 (1995).

[14] R. N.Thurston, J. P. Heritage, A. M. Weiner and W. J. Tomlinson, IEEE J. Quantum Electron, **22,** 682–696 (1986).

[15] D. Meshulach, D. Yelin, and Y. Silberberg, Opt. Commun. **138,** 345–348 (1997).

[16] D. Meshulach, D. Yelin, Y. Silberberg, J. Opt. Soc. Am. B **155,** 1615–1619 (1998).

[17] A. M. Weiner, S. Oudin, D. E. Leaird, D. H. Reitze, J. Opt. Soc. Am. B **105,** 1112-1120 (1993).

[18] W. Koechner, *Solid State Laser Engineering* (Springer, 1999).